What to see and what not to see in three-photon absorption: (3+1) REMPI of HBr

Ágúst Kvaran,[a] Benedikt G. Waage, and Huasheng Wang
Science Institute, University of Iceland, Dunhaga 3, 107 Reykjavík, Iceland

(Received 11 January 2000; accepted 3 May 2000)

Hönl–London type approximation expressions are derived for transition strengths of the $\Omega'=0,1,2,3, \leftarrow\Omega''=0$ (Σ, Π, Δ and $\Phi\leftarrow\Sigma$) three-photon transitions for diatomic molecules belonging to Hund's case (a) and intermediate (a)–(b) coupling schemes. These are used to demonstrate what may be seen and what may not be seen in three-photon absorption spectra. The forms are used to simulate room temperature (3+1)REMPI spectra of HBr, for different electronic transitions. The analysis as well as comparison with (2+1)REMPI spectra is used to demonstrate the usefulness of three-photon absorption spectroscopy to identify excited states and to derive spectroscopic parameters. A Rydberg state, not observed in single or two-photon absorption, with band origin 82 837 cm^{-1} was identified and analyzed for the first time. It was assigned as the $L^1\Phi(3)$ $((\sigma^2\pi^3)5d\delta)$ state, (0,0) band. © *2000 American Institute of Physics.* [S0021-9606(00)00929-6]

INTRODUCTION

Although single-photon absorption has dominated in high-resolution spectroscopy throughout the years, one-color multiphoton absorption has gained increasing importance recently as LASERS have become more commonly available.[1] Thus, for example, rotational (2+1) REMPI spectroscopy of the halogens,[2–7] interhalogens[2,8] and the hydrogen halides,[2,9–18] which has been emphasized in our laboratory recently,[2–9] has proved to be very useful in this respect. Advantages of using multiphoton absorption methods instead of classical single-photon absorption methods in electronic spectroscopy are associated with (i) different selection rules and (ii) use of lower energy photons in particular. Since the total angular momentum of a molecule can increase with the number of absorbing photons, more and/or different states can be accessed as the number of absorbing photons increases. Lower energy, yet higher density, LASER radiation with a larger flux of lower energy photons can sometimes replace synchrotron sources which, while more difficult to operate, are frequently used in single-photon excitation studies in the VUV spectral region.

While the use of one-color two-photon absorption has become common in high-resolution spectroscopy recently, the same cannot be said about the use of one-color three-photon absorption. Most high-resolution spectroscopy work involving three-photon absorption has been done by using the REMPI technique for small gas phase molecules, such as H_2,[19] O_2,[20] CO_2,[21,22] CS_2,[23–25] and Cl_2.[26] Both single[27] and two-photon[28] absorption spectra studies of diatomic molecules primarily make use of simple Hönl–London type expressions for line strengths which allow selection rules and spectra line intensities to be evaluated.

In this paper we present simplified and useful Hönl–London type approximation expressions for rotational line strengths for electronic transitions from a $\Omega''=0$ (alternatively Σ) state to $\Omega'=0$, 1, 2 and 3 (alternatively Σ, Π, Δ and Φ) states. This is of relevance to the work on the halogen containing compounds mentioned above. The expressions of concern are derived from more general ones given by Halpern *et al.*[29] These are used to demonstrate what may be seen and what may not be seen in three-photon absorption spectra due to electronic transitions from of $\Omega''=0$ (Σ) ground state molecules. Furthermore (3+1)REMPI and (2+1)REMPI spectra for HBr are compared and/or simulated, using the expressions for the rotational line strengths.

EXPERIMENT

The apparatus used has been described in detail elsewhere[2–4] so only a brief report will be given here. Tunable radiation was generated by an excimer laser-pumped dye laser system. For wavelengths less than about 330 nm, the laser output was frequency doubled by suitable SHG crystals. The frequency-doubled beam was separated from the fundamental by a Pellin Broca prism. The radiation was focused into an ionization cell between two electrodes. The cell contained gas samples at low pressure, typically $\leqslant$5 Torr. Current pulses in the gas due to laser pulse photoionization caused voltage drops across the electrodes. After amplification and integration the voltage pulses were fed into a multichannel analyzer for peak height measurements and recording. Finally average pulse heights for a fixed sampling time were recorded to get the spectrum. Typically spectral points were obtained by averaging over 100 pulses. The bandwidth of the dye laser beam was about 0.05 cm^{-1}. Care was taken to prevent power broadening due to ac Stark effects by minimizing laser power. Wavelength calibration was

[a]Correspondence should be addressed to: Ágúst Kvaran; Permanent address: Science Institute, University of Iceland, Dunhaga 3, 107 Reykjavík, Iceland, Phone: +354-525-4800, Fax: +354-552-8911, E-mail: agust@raunvis.hi.is, Home page: http://www.raunvis.hi.is/~agust/

achieved by recording chlorine, bromine and iodine[30] atomic lines or by comparison of the strongest hydrogen chloride rotational lines with those reported by Green *et al.*[15] The accuracy of the calibration was found to be about ± 2 cm^{-1} on the two- and three-photon wave number scales. Spectra intensities were corrected for possible intensity drift during the scan. Furthermore, the effect of varying LASER power was corrected for by dividing the measured intensity by the power cubed for (3+1)REMPI spectra and by the power squared for (2+1)REMPI spectra.

THEORY AND SPECTRA STRUCTURE

The one color three-photon transition probability (σ), can be expressed as[29,31]

$$\sigma \propto \left| \sum_{i1,i2} \frac{\langle \psi_1 | \overline{\mathbf{M}} \cdot \overline{\mathbf{E}} | \psi_{i2} \rangle \langle \psi_{i2} | \overline{\mathbf{M}} \cdot \overline{\mathbf{E}} | \psi_{i1} \rangle \langle \psi_{i1} | \overline{\mathbf{M}} \cdot \overline{\mathbf{E}} | \psi_0 \rangle}{(\omega_{i2,0} - \omega)(\omega_{i1,0} - 2\omega)} \right|, \quad (1)$$

where ψ_0, ψ_{i1}, ψ_{i2} and ψ_1 are the wave functions for the ground state (ψ_0), two virtual intermediate states (ψ_{i1}, ψ_{i2}) and the resonance excited state (ψ_1). ω is the photon frequency and $\omega_{i1,0}$ and $\omega_{i2,0}$ are the frequencies corresponding to the energy-differences between the ground state and the two virtual intermediate states, $i1$ and $i2$, respectively. The operators are the inner products of the molecular dipole moments, **M**, and the electric field of the exciting light, **E**.

Approximate expressions for three-photon absorption line strengths ($S_{\Delta\Omega}$), for linearly polarized light, have been derived from Eq. (1) for diatomic molecules belonging to Hund's case (a) and intermediate (a)–(b) coupling schemes.[29] The approximation is based on the assumptions that (i) the denominator in Eq. (1) changes insignificantly with frequency, corresponding to largely off-resonance intermediate virtual states and (ii) that intermediate virtual states of the same symmetry are replaced by a single representative state. The general formulas for the three-photon absorption strength are of the form

$$S_{\Delta\Omega} = s_1 \mu_1^2 + s_3 \mu_3^2, \quad (2)$$

where s_1 and s_3 are functions of the ground and the excited states total angular momentum quantum numbers (J'' and J') as well as the total electronic angular momentum projection quantum numbers (Ω'' and Ω'). The expressions for s_1 and s_3, given by Halpern *et al.*,[29] are written in terms of Clebsch–Gordan coefficients (transformation amplitudes) of the form $(J'j - \Omega' \pm (\Omega' - \Omega'')|J'' - \Omega'')$ for $j=1$ (i.e., first order coefficients[32]) and $j=3$ (third order coefficients[33]), respectively. μ_1^2 and μ_3^2 are sum and product functions of $\mu_\parallel$ and $\mu_\pm$ values [see Eqs. (29a)–(29d) given by Halpern *et al.*[29])], which represent the collective effect of all one photon transition moments and energy denominators that give rise to parallel or perpendicular transitions, respectively,

$$\mu_\parallel = \langle \Omega | \overline{\mathbf{M}} \cdot \overline{\mathbf{E}} | \Omega \rangle, \quad (3a)$$

$$\mu_\pm = \langle \Omega \pm 1 | \overline{\mathbf{M}} \cdot \overline{\mathbf{E}} | \Omega \rangle. \quad (3b)$$

Although these parameters can, in principle, be measured from spectra, in some cases, treating these as variables or fitting parameters is more appropriate. We have carried the expressions for the three-photon absorption strength, as given by Halpern *et al.*,[29] a step further by substituting the Clebsch–Gordan coefficients by its counterpart functions of J', J'', Ω' and Ω'' (Refs. 32, 33) for $\Omega''=0$, $\Omega'=0$, 1, 2 and 3 and for different rotational series, $N(J'=J''-3)$ to $T(J'=J''+3)$ (see Table I). Valid regions and regions of nonzero values for the expressions are specified in the table. These approximation expressions are particularly suitable for direct evaluation of rotational line intensities as functions of J'' ($=J$ in Table I) and allow easy investigation of selection rules.

From Table I, it is clear that only *N*, *P*, *R* and *T* lines (not *O*, *Q* and *S* lines) will be seen for Σ–Σ three-photon transitions. In the case of a zero μ_3^2 value (i.e., $S_{\Delta\Omega} = s_1 \mu_1^2$) only *P* and *R* branches with the same line strengths as in single-photon absorption spectra will be seen.[27] For the other transitions (Π, Δ, $\Phi \leftarrow \Sigma$) all rotational line series (*N* to *T*) can be expected to be seen, while in the case of the $\Pi \leftarrow \Sigma$ transition a spectrum showing *P*, *Q* and *R* lines only, as in single-photon absorption, will be seen in the case of a zero μ_3^2 value.

The structure of the three-photon strength can be seen from diagrams of the type shown in Fig. 1 for the Σ^+–Σ^+ transition. The intermediate states of a given type are shown as dashed lines (one line for each group of electronic states that can enter into the process) and the possible transitions are drawn by using well-known one-photon selection rules. More detailed analysis of the *J* dependence of individual transitions is helpful in organizing the various terms that contribute to the amplitude.[34] Thus, from selection rules for single-photon transitions, it can be seen directly that a Σ^+–Σ^+ transition only displays *N*, *P*, *R* and *T* lines and cannot display *O*, *Q* and *S* branches. It can also be found out, by multiplying the number of exit (absorbing) lines by the number of entrance lines for each virtual state (each broken line on the figure), that the *P* and the *R* branch transition strengths contain 17 terms each, and that the *N* and the *T* branch amplitudes each have 4 terms. Thus, the four channels leading to *N* lines are:

(1) $\Sigma^+(1;J-3) \leftarrow \Sigma^+(i2;J-2) \leftarrow \Sigma^+(i1;J-1) \leftarrow \Sigma^+(0,J)$,

(2) $\Sigma^+(1;J-3) \leftarrow \Pi_-(i2;J-2) \leftarrow \Sigma^+(i1;J-1) \leftarrow \Sigma^+(0,J)$,

(3) $\Sigma^+(1;J-3) \leftarrow \Sigma^+(i2;J-2) \leftarrow \Pi_-(i1;J-1) \leftarrow \Sigma^+(0,J)$,

(4) $\Sigma^+(1;J-3) \leftarrow \Pi_-(i2;J-2) \leftarrow \Pi_-(i1;J-1) \leftarrow \Sigma^+(0,J)$.

The relative line strengths of the various line series for dominant first order ($S_{\Delta\Omega} = s_1 \mu_1^2$; $\Sigma, \Pi \leftarrow \Sigma$) and third order ($S_{\Delta\Omega} = s_3 \mu_3^2$; $\Sigma, \Pi, \Delta, \Phi \leftarrow \Sigma$) contributions are listed in Table II. These ratios are derived from the limit values of the relevant expressions in Table I as *J* goes to infinity.

In order to calculate or simulate a three-photon absorption spectrum, line *positions* as well as line *intensities* need

TABLE I. Three-photon rotational line strengths, $S_{\Delta\Omega}=s_1\mu_1^2+s_3\mu_3^2$ for the transitions $\Omega'\leftarrow\Omega''=0$; $\Omega'=0,1,2,3$ ($\Sigma,\Pi,\Delta,\Phi\leftarrow\Sigma$). s_1 and s_3 are expressed as functions of J ($=J''$) shown below and μ_1^2 and μ_3^2 are defined by Halpern *et al.* (Ref. 29) and were treated as variables in our simulation calculations (see text). Valid regions and regions of nonzero values for the s_1 and s_3 functions are indicated. Lowest J numbers to be observed in each rotational line serie are highlighted in bold.

Rot. line series\s_i	$\Omega'=0(\Sigma)$		$\Omega'=1(\Pi)$		$\Omega'=2(\Delta)$[a]	$\Omega'=3(\Phi)$[a]
	s_1	s_3	s_1	s_3	s_3	s_3
$N(J-3\leftarrow J;$ $J\geqslant 3)$	0	$\frac{1}{70}\frac{(J-2)(J-1)J}{(2J-3)(2J-1)}$ **$J\geqslant 3$**	0	$\frac{1}{70}\frac{(J-1)J(J-3)}{(2J-3)(2J-1)}$ **$J\geqslant 4$**	$\frac{1}{70}\frac{J(J-4)(J-3)}{(2J-3)(2J-1)}$ **$J\geqslant 5$**	$\frac{1}{70}\frac{(J-5)(J-4)(J-3)}{(2J-3)(2J-1)}$ **$J\geqslant 6$**
$O(J-2\leftarrow J;$ $J\geqslant 2)$	0	0	0	$\frac{1}{210}\frac{(J+1)J}{(2J-1)}$ **$J\geqslant 3$**	$\frac{2}{105}\frac{(J+1)(J-3)}{(2J-1)}$ **$J\geqslant 4$**	$\frac{3}{70}\frac{(J-4)(J-3)}{(2J-1)}$ **$J\geqslant 5$**
$P(J-1\leftarrow J;$ $J\geqslant 1)$	$\frac{1}{27}J$ **$J\geqslant 1$**	$\frac{3}{350}\frac{(J-1)J(J+1)}{(2J+3)(2J-3)}$ $J\geqslant 2$	$\frac{1}{27}(J-1)$ **$J\geqslant 2$**	$\frac{1}{1050}\frac{(J+1)(J-6)^2}{(2J+3)(2J-3)}$ $6>J\geqslant 2;$ $J\geqslant 7$	$\frac{1}{42}\frac{(J+3)^2(J-2)}{(2J+3)(2J-3)}$ **$J\geqslant 3$**	$\frac{3}{14}\frac{(J-3)(J-2)(J+2)}{(2J+3)(2J-3)}$ **$J\geqslant 4$**
$Q(J\leftarrow J;$ $J\geqslant 0)$	0	0	$\frac{1}{27}(2J+1)$ **$J\geqslant 1$**	$\frac{1}{175}\frac{(2J+1)(J-1)(J+2)}{(2J+3)(2J-1)}$ $J\geqslant 2$	$\frac{1}{7}\frac{(2J+1)}{(2J+3)(2J-1)}$ **$J\geqslant 2$**	$\frac{1}{7}\frac{(2J+1)(J-2)(J+3)}{(2J+3)(2J-1)}$ **$J\geqslant 3$**
$R(J+1\leftarrow J;$ $J\geqslant 0)$	$\frac{1}{27}(J+1)$ **$J\geqslant 0$**	$\frac{3}{350}\frac{J(J+1)(J+3)}{(2J-1)(2J+5)}$ $J\geqslant 1$	$\frac{1}{27}(J+2)$ **$J\geqslant 0$**	$\frac{1}{1050}\frac{J(J+7)^2}{(2J-1)(2J+5)}$ $J\geqslant 1$	$\frac{1}{42}\frac{(J-2)^2(J+3)}{(2J-1)(2J+5)}$ $J=$**1**, $J\geqslant 3$	$\frac{3}{14}\frac{(J+4)(J+3)(J-1)}{(2J-1)(2J+5)}$ **$J\geqslant 2$**
$S(J+2\leftarrow J;$ $J\geqslant 0)$	0	0	0	$\frac{1}{210}\frac{J(J+1)}{(2J+3)}$ **$J\geqslant 1$**	$\frac{2}{105}\frac{J(J+4)}{(2J+3)}$ **$J\geqslant 1$**	$\frac{3}{70}\frac{(J+5)(J+4)}{(2J+3)}$ **$J\geqslant 1$**
$T(J+3\leftarrow J;$ $J\geqslant 0)$	0	$\frac{1}{70}\frac{(J+1)(J+2)(J+3)}{(2J+5)(2J+3)}$ **$J\geqslant 0$**	0	$\frac{1}{70}\frac{(J+4)(J+2)(J+1)}{(2J+5)(2J+3)}$ **$J\geqslant 0$**	$\frac{1}{70}\frac{(J+5)(J+4)(J+1)}{(2J+5)(2J+3)}$ **$J\geqslant 0$**	$\frac{1}{70}\frac{(J+6)(J+5)(J+4)}{(2J+5)(2J+3)}$ **$J\geqslant 0$**

[a]$s_1=0$ for all rotational line series.

to be calculated. Line *positions* for rovibrational lines ($\nu_{J',v'\leftarrow J'',v''}/\mathrm{cm}^{-1}$) can be expressed as

$$\nu_{J',v'\leftarrow J'',v''}=\nu^o_{v',v''}+\Delta\overline{E}_{J',J''}, \tag{4}$$

where $\nu^o_{v',v''}$ is the band origin (in cm^{-1}) of a vibrational band. $\Delta E_{J',J''}$ is the difference in rotational energies (in cm^{-1}), depending on the rotational parameters (B', D', B'' and D'') and the rotational quantum numbers (J',J'') for the two states as

$$\Delta\overline{E}_{J'J''}=(J+\Delta J)(J+\Delta J+1)B'-(J+\Delta J)^2\times(J+\Delta J+1)^2D'-J(J+1)B''+J^2(J+1)^2D'', \tag{5}$$

where $J=J''$ and $\Delta J=J'-J''$. The relative rotational line

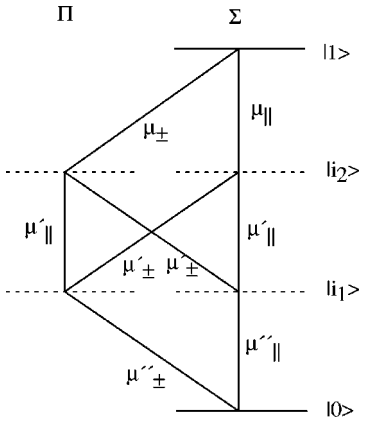

FIG. 1. Structure of the three-photon transition amplitude for a diatomic molecule showing intermediate/virtual states and one-photon transition moments for Σ–$\Sigma(\Omega=0-\Omega=0)$ overall transitions.

TABLE II. The intensity ratios of the line series for the cases when the transition strength, $S_{\Delta\Omega}=s_1\mu_1^2$, $\Omega'=0$, $1\leftarrow\Omega''=0$ ($\Sigma,\Pi\leftarrow\Sigma$) and $S_{\Delta\Omega}=s_3\mu_3^2$, $\Omega'=0,1,2,3\leftarrow\Omega''=0$ ($\Sigma,\Pi,\Delta,\Phi\leftarrow\Sigma$) for three-photon absorptions.

Transition	Absorption strengths	N	O	P	Q	R	S	T
$\Sigma\leftarrow\Sigma$	$s_1\mu_1^2$	0	0	1	0	1	0	0
$\Sigma\leftarrow\Sigma$	$s_3\mu_3^2$	5	0	3	0	3	0	5
$\Pi\leftarrow\Sigma$	$s_1\mu_1^2$	0	0	1	2	1	0	0
$\Pi\leftarrow\Sigma$	$s_3\mu_3^2$	15	10	1	12	1	10	15
$\Delta\leftarrow\Sigma$	$s_3\mu_3^2$	3	8	5	0	5	8	3
$\Phi\leftarrow\Sigma$	$s_3\mu_3^2$	1	6	15	20	15	6	1

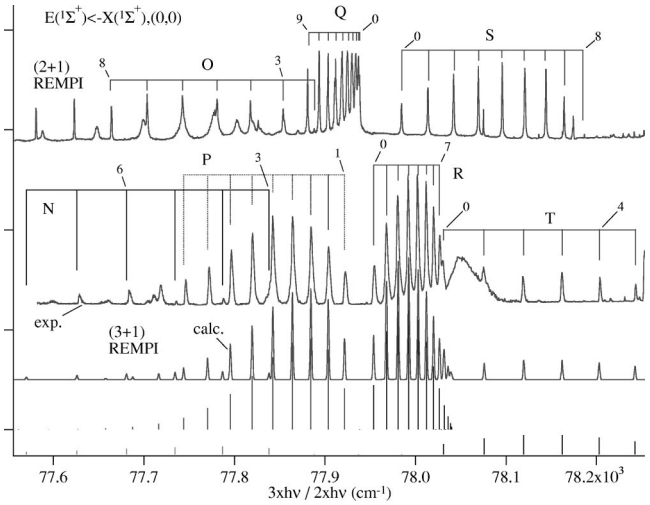

FIG. 2. HBr, $E(^1\Sigma^+)\leftarrow X(^1\Sigma^+)$, (0,0) spectra analysis: Observed (2+1)REMPI spectrum (top), observed (3+1)REMPI spectrum(below), calculated rotational line contributions (bottom) and simulated spectrum (underneath exp. spectra). Rotational line numbers are J'' values. The $V(^1\Sigma^+)-X(^1\Sigma^+)$ ($v'=m+4,0$; Q lines) spectrum overlaps partly in the (2+1)REMPI spectrum (77 840–77 580 cm^{-1}). The sharp line at 78 069.3 cm^{-1} is a bromine atomic line (two-photon transition $^4P^o_{1/2}\leftarrow{}^2P^o_{3/2}$). The broad feature near 78 060 cm^{-1} in the (3+1)REMPI spectrum is of unknown origin.

intensities (I_{rel}), for a vibrational band are proportional to the product of the Boltzmann population and the three-photon absorption strength, $S_{\Delta\Omega}$

$$I_{rel}=CS_{\Delta\Omega}\exp(-\overline{E}(J'')hc/kT). \quad (6)$$

Finally rotational lines are either displayed as lines from zero or as Gaussian-shaped functions for specified bandwidths. Calculated spectra for three-photon absorption, relevant to (3+1)REMPI of HBr are to be found on the Web.[34]

The following main characteristics of three-photon absorption spectra can be derived from calculated spectra and/or Tables I and II:

(a) $\Omega'=0\leftarrow\Omega''=0(\Sigma\leftarrow\Sigma)$ (see Fig. 2):
(i) No *O,Q,* and *S* lines are to be observed.
(ii) Only *P* and *R* lines are to be observed if $\mu_3^2=0$.
(iii) The ratio of the *N* and *T* lines over the *P* and *R* lines ($I(N,T)/I(P,R)$) increases as μ_1^2/μ_3^2 decreases [see Eq. (2)].
(iv) The relative intensities of the first rotational lines in the *P* and the *R* line series ($J''=1$ and 0, respectively) drop as μ_1^2/μ_3^2 decreases and equal zero for $\mu_1^2=0$.

(b) $\Omega'=1\leftarrow\Omega''=0(\Pi\leftarrow\Sigma)$ (see Fig. 3):
(i) The ratio of the *N, O, Q, S* and *T* lines over the *P* and *R* lines ($I(N,O,Q,S,T)/I(P,R)$) increases as μ_1^2/μ_3^2 decreases.
(ii) The relative intensity of the first rotational line in the *R* series ($J''=0$) drops to zero as μ_1^2/μ_3^2 decreases.
(iii) the rotational line $J'=2\leftarrow J''=0(S)$ is not expected to be seen.

(c) $\Omega'=2\leftarrow\Omega''=0(\Delta\leftarrow\Sigma)$:
(i) The *Q* line intensities are weak and decrease rapidly with increasing *J*.
(ii) The rotational line for $J''=0$ in the *S* series is not expected to be seen.
(iii) The rotational line for $J''=1$ in the *R* series sticks out and the line for $J''=2$ is not expected to be seen.

(d) $\Omega'=3\leftarrow\Omega''=0(\Phi\leftarrow\Sigma)$ (see Fig. 4):
(i) The *S* and the *T* line series show characteristic overall drop in intensity (for room temperature) with *J* starting from its first line ($J''=1$ for *S* and $J''=0$ for *T*).
(ii) Characteristic large gap between the first rotational lines in the *Q* line series and those in the *P* or *R* line series is expected to be seen.

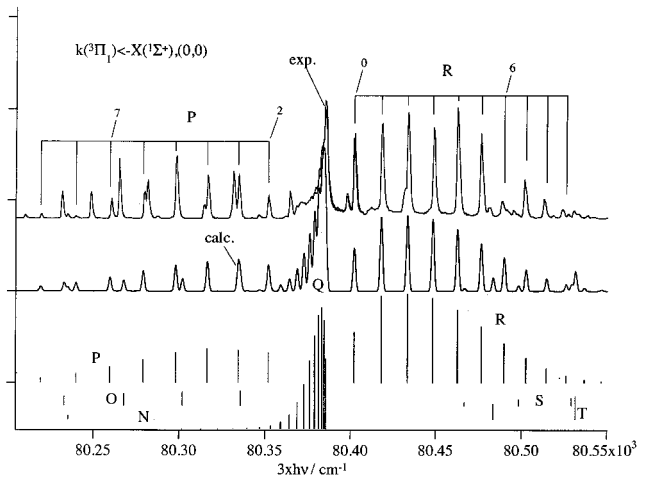

FIG. 3. HBr, $k(^3\Pi_1(1))\leftarrow X(^1\Sigma^+)$, (0,0) (3+1)REMPI spectrum analysis: Observed (3+1)REMPI spectrum (top), calculated rotational line contributions (bottom) and simulated spectrum (underneath exp. spectrum). Rotational line numbers are J'' values. Some overlapping spectra features, yet unassigned, are observed in the region 80 200–80 400 cm^{-1}.

RESULTS AND ANALYSIS

(3+1)REMPI spectra for HBr (ionization potential $=94\,125$ cm^{-1}) might be expected to be observed in the

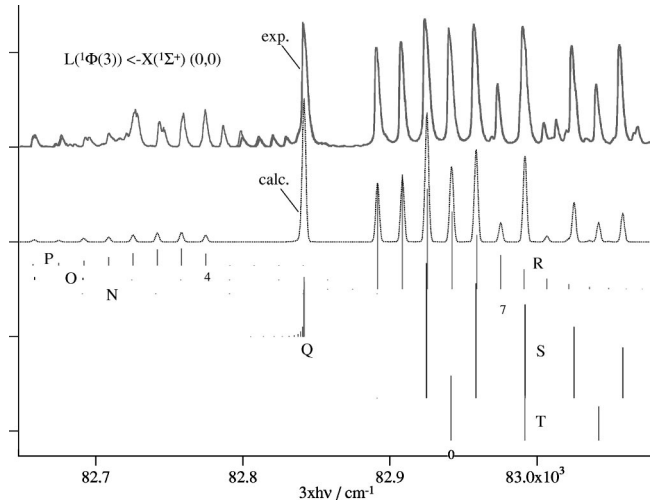

FIG. 4. HBr, $L(^1\Phi(3))\leftarrow X(^1\Sigma^+)$, (0,0) (3+1)REMPI spectrum analysis: Observed (3+1)REMPI spectrum (top), calculated rotational line contributions (bottom) and simulated spectrum (underneath exp. spectrum). Rotational line numbers are J'' values. Some unidentified overlapping spectrum is to be found in the region 82 650–82 830 cm^{-1}.

TABLE III. $H^{81}Br$: Band origins (ν^0) and rotational parameters (B' and D') for states analyzed by simulations of (3+1)REMPI ($E(^1\Sigma^+),H(^1\Sigma^+),k(^3\Pi_1(1)),L^1\Phi(3)$) and (2+1)REMPI ($E(^1\Sigma^+),H(^1\Sigma^+)$) spectra.

HBr				ν^0		B'/cm^{-1}		$D'\times10^3/\text{cm}^{-1}$		Ref.
State	Configurations:	Ion core	v'	Our work	Other work	Our work	Other work	Our work	Other work	Other work
$E(^1\Sigma^+)$	$(\sigma^2\pi^3)5p\pi$	$^2\Pi_{1/2}$	0	77 933±2	77 939.5	7.72±0.04	7.721	0.3±0.1	0.3	16
$H(^1\Sigma^+)$	$(\sigma^2\pi^3)5d\pi$	$^2\Pi_{3/2}$	0	79 640±2	79 646.3	7.015±0.040	7.029	−2.6±0.1	−3.3	36
					79 645.5		7.193		0.6	16
$k(^3\Pi_1(1))$	$(\sigma^2\pi^3)5d\delta$	$^2\Pi_{3/2}$	0	80 379±3	80 386	8.125±0.050[a]	8.13	0.5±0.1	0.07	36
$L(^1\Phi(3))$	$(\sigma^2\pi^3)5d\delta$	$^2\Pi_{1/2}$	0	82 837±3		8.39±0.05		0.85±0.10		

[a]Values for the + and − components were found to be identical within experimental uncertainties.

wavelength region 319–425 nm, corresponding to the resonance excitation region 64 590–94 125 cm^{-1}. We scanned the region 77 000–86 200 cm^{-1} (348–390 nm LASER excitation). The same excitation region was scanned in order to record (2+1)REMPI spectra (232–260 nm.) The region above 83 200 cm^{-1} in (3+1)REMPI shows very rich and complicated structure while the region below this limit, although showing some overlap of spectra, was found to be more accessible for analysis. As a first guide toward analysing vibrational bands we found it very useful to plot up values of spacings between neighboring rotational peaks ($\Delta v_{J,J+1}$) as a function of integer number (n) and to compare these with the first order approximation equations ($D'=D''=0$) for the spacing values as a functions of J quantum numbers

$$\Delta v_{J,J+1}=2(B'-B'')J+2(\{\Delta J+1\}B'-B''), \tag{7}$$

where $J=J''$ and $\Delta J=J'-J$ ($\Delta J=-3$ for N lines, -2 for O lines, etc.). These expressions are linear functions of J with slope values independent of rotational line series ($2(B'-B'')$), which allows an easy estimate of (i) the B' constants for known B'' and (ii) intercept values for the various line series. Afterwards J quantum numbers could be evaluated to assign rotational lines. In what follows we will describe analysis of two Σ–Σ spectra bands both observed and recorded in (3+1) and (2+1)REMPI as well as one Π–Σ and one Φ–Σ system observed in (3+1)REMPI.

$E(^1\Sigma^+)\leftarrow X(^1\Sigma^+)$, (0,0)

Figure 2 shows (2+1) (top) and (3+1) (below) REMPI spectra in the excitation region 77 500–78 300 cm^{-1}. The main features of the spectra can be assigned to the $E(^1\Sigma^+)\leftarrow X(^1\Sigma^+)$, (0,0) system which has been seen before, both in single-photon absorption[35] and in (2+1) REMPI.[9,16] The (2+1)REMPI spectrum also shows Q lines due to the $V(^1\Sigma^+)\leftarrow X(^1\Sigma^+)$ ($v'=m+4,0$) system[9] in the 77 800–77 500 cm^{-1} region. Furthermore, some unidentified broad feature is seen in the (3+1)REMPI spectrum near 78 060 cm^{-1}. The $E(^1\Sigma^+)\leftarrow X(^1\Sigma^+)$ spectrum shows clear rotational line series: (i) O, Q and S branches in (2+1)REMPI and (ii) N, P, R and T branches in (3+1) REMPI. These observations are in agreement with expectations: Observed and absent rotational line series follow the selection rules given by Bray and Hochstrasser[28] for two-photon absorption and above for three-photon absorption. The intensity structure of the (2+1)REMPI spectrum broadly follows the predicted intensity based on the transition strength expressions derived by Bray and Hochstrasser[28] as shown by Kvaran *et al.*[9] At the bottom of Fig. 2 are shown calculated rotational line contributions to the (3+1)REMPI spectrum obtained by using the calculation procedure described above. A simulated spectrum is shown directly underneath the experimental spectrum.

Simultaneous simulations of the (2+1) and (3+1)REMPI spectra revealed the spectroscopic parameters listed in Table III along with values obtained by others. The determination of these parameters is solely based on the comparison of the *positions* of calculated and experimental rotational lines, but independent of line *intensities* as seen by inspections of Eqs. (4) and (5). The simulation procedure was carried out by a least squares analysis technique. The relative intensities of the rotational lines in both spectra are determined by Eq. (6) for the (3+1)REMPI spectrum and by an analogous expression for the (2+1)REMPI spectrum.[9] The only adjustable fit parameters are μ_1^2 and μ_3^2 in the former case and analogous parameters (μ_I^2 and μ_S^2) in the latter case.[9] The main effect of changing the ratio of these parameters is to change the relative intensities of line series $(I(N,T)/I(P,R)$ in (3+1)REMPI as mentioned above and $I(O,S)/I(Q)$ in (2+1)REMPI[9]) and to a lesser extent, to change the relative intensities within the line series. In order to obtain the best relative intensities of line series in the (3+1)REMPI simulation a ratio of $\mu_1^2:\mu_3^2=2:3$ was used ($\mu_1^2:\mu_S^2=3:20$ was used in the (2+1)REMPI spectrum[9,16]). In both spectra the ratio of experimental to calculated rotational line intensities is found to increase with J quantum number for all line series. There could be two explanations for this effect: (i) Either the approximate expressions for the line strengths (Table I) are not fully appropriate to describe the line intensities due to break down of the approximations involved (see above) and/or (ii) a well known perturbative interactions between the E Rydberg state and the $V(^1\Sigma^+)$ ion-pair state[9] could be the cause of this. Since an analogous effect does not seem to be equally large in the next neighbor Σ-Rydberg state spectrum for the $H(^1\Sigma^+)$ state ($\nu^0=79\,640\,\text{cm}^{-1}$; see below), which is not found to interact strongly with the $V(^1\Sigma^+)$ state, we feel that the latter explanation is more likely. The intensity structure of the line series broadly follows the predicted intensity based on the transition strength expressions (Table I).

$H(^1\Sigma^+) \leftarrow X(^1\Sigma^+)$, (0,0)

The main features of the spectra in the excitation region 79 200–79 850 cm^{-1} can be assigned to the $H(^1\Sigma^+) \leftarrow X(^1\Sigma^+)$, (0,0) system, which has been observed both in single-photon absorption[36] and (2+1)REMPI.[16,37] Q branch lines due to the $V(^1\Sigma^+) \leftarrow X(^1\Sigma^+)$ ($v' = m + 7,0$) system as well as S branch lines due to the $F(^1\Delta(2)) \leftarrow X(^1\Sigma^+)$ (1,0) system overlap in the region of the O lines in the (2+1)REMPI spectrum. Spectroscopic parameters derived from simultaneous simulations of (3+1) and (2+1)REMPI spectra are listed in Table III along with values derived by others. $\mu_1^2:\mu_3^2 = 2:3$ was used in the simulation of the (3+1)REMPI spectrum, while $\mu_I^2:\mu_S^2 = 1:6$ was used for the (2+1)REMPI spectrum. The spectra follow closely the theoretical predictions in terms of line intensities and selection rules analogous to those found for the $E \leftarrow X$ spectrum as mentioned above.

$k(^3\Pi_1(1)) \leftarrow X(^1\Sigma^+)$, (0,0)

Figure 3 shows the (3+1)REMPI spectrum in the excitation region 80 200–80 550 cm^{-1}. The main features of the spectrum can be assigned to the $k(^3\Pi_1(1)) \leftarrow X(^1\Sigma^+)$, (0,0) system, which has been observed in single-photon absorption.[36] Some overlapping spectral features, yet unassigned, are observed on the low wave number side of the Q branch. The spectrum shows clear P, Q and R line series, while other rotational line series (N, O, S and T) are much weaker or undetectable. Calculated rotation contributions and a simulated spectrum are also shown in the figure for the rotational parameters listed in Table III. The calculated spectra were derived for $\mu_1^2:\mu_3^2 = 1:1$, but spectra for virtually undetectable N, O, S and T line series but unchanged structure of the P, Q and the R series could be obtained for $\mu_1^2:\mu_3^2 \geqslant 1$.

$L(^1\Phi(3)) \leftarrow X(^1\Sigma^+)$, (0,0)

Figure 4 shows the (3+1)REMPI spectrum in the excitation region 82 650–83 100 cm^{-1}. The main features of the spectrum could be explained as being due to a $\Omega' = 3 \leftarrow \Omega'' = 0 (\Phi \leftarrow \Sigma)$ transition as shown by a comparison with the simulated spectrum and the calculated rotational contributions (Fig. 4). Some unidentified overlapping spectrum is found in the region 82 650–82 830 cm^{-1}. A large gap is observed between the Q branch and the first rotational band on its high wave number side as to be expected for a $\Phi \leftarrow \Sigma$ spectrum, since R lines for transitions from $J = 0$ and 1 will not be seen. The Q branch peak is particularly sharp, suggesting that the rotational constant for the upper state closely resembles the one for the ground state. In such a case rotational lines will overlap in a characteristic way, so that peaks in the S line series will overlap every other peak in the R branch and peaks in the T line series will overlap every third peak in the R branch. Similar holds for the peaks in the N, O and P line series. Intensity alterations in the observed spectra show reasonably good agreement with the prediction made by using the approximation expressions described above. Spectroscopic parameters derived from the simulation are listed in Table III.

The upper state for this system has not been observed/assigned before. Three of four Rydberg states belonging to the $d\delta$ manifold ($(\sigma^2\pi^3)5d\delta$) and diverging to the ground state ion ($^2\Pi_{1/2}$) have been reported in this spectral area, i.e., the $k^3\Pi_2(2)$ ($\nu^0 = 82\,676.9\ cm^{-1}$),[36] $K^1\Pi(1)$ ($\nu^0 = 83\,453\ cm^{-1}$)[16,36] and $l^3\Phi_2(2)$ ($\nu^0 = 82\,583\ cm^{-1}$).[16] The remaining state, which belongs to this category and which is expected to be found in this region is the $L^1\Phi(3)$ state, which is not accessible by single and two-photon absorption. There is also a reason to believe that a singlet state will have relatively high transition probability. The similarity in rotational parameters observed for this state and the ground state, hence comparable average internuclear distances for the two potential curves, suggests that the (0,0) band will be the dominant vibrational band. We therefore assign this band to $L^1\Phi(3)$, (0,0).

CONCLUSIONS

Easy to use, expressions for transition strengths of three-photon absorptions due to $\Omega' = 0,1,2,3 \leftarrow \Omega'' = 0$ (alternatively: $\Sigma, \Pi, \Delta, \Phi \leftarrow \Sigma$) transitions of diatomic molecules are presented in this paper. Characteristics of the corresponding three-photon absorption rovibrational spectra are discussed and demonstrated with reference to Rydberg excitation in HBr. (3+1) and (2+1) REMPI spectra of HBr were recorded at room temperature over the spectral region 77 000–86 200 cm^{-1}. Useful guidelines for first step analysis of rotational structure are given. Both (3+1) and (2+1)REMPI show spectra due to the $E(^1\Sigma^+) \leftarrow X(^1\Sigma^+)$, (0,0) and the $H(^1\Sigma^+) \leftarrow X(^1\Sigma^+)$, (0,0) transitions, while the $k(^3\Pi_1(1)) \leftarrow X(^1\Sigma^+)$, (0,0) transition is only observed in (3+1) REMPI. These were simulated to demonstrate the usefulness of the transition strengths for spectra analysis and to derive spectroscopic parameters for the excited states involved. Good agreement is found between (2+1) and (3+1)REMPI spectra and with others data in terms of evaluated rotational parameters. Band origins for the $E(0,0)$, $H(0,0)$ and $k(0,0)$ bands are found to be slightly, but significantly, lower than what is reported in the literature (see Table III). A (3+1)REMPI spectrum due to a $\Omega' = 3 \leftarrow \Omega'' = 0$ ($\Phi \leftarrow \Sigma$) transition at $\nu^o = 82\,837\ cm^{-1}$ was observed for the first time. Simulation of the spectrum allowed evaluations of spectroscopic constants for the newly observed state, which is assigned as the $L^1\Phi(3)$ Rydberg state and the (0,0) vibrational band. This state has the electronic configuration $(\sigma^2\pi^3)5d\delta$ and ion core term symbol $^2\Pi_{1/2}$. Generally (3+1)REMPI spectra, along with expressions for three-photon line strengths, are found to be useful spectroscopic tools, either by supporting and adding to observations obtained by other methods or in order to explore new territories and identifying new excited states.

ACKNOWLEDGMENTS

The financial support of the University Research Fund, University of Iceland and the Icelandic Science Foundation

is gratefully acknowledged. We thank Dr. Lars Madsen (Max–Planck-Institut, Garching) for useful discussions and important help with theoretical analysis. A.K. thanks Professor J.C. Polanyi for his support during his stay at the Chemistry Department, University of Toronto.

[1] M. Hollas, *High Resolution Spectroscopy*, 2nd ed. (Wiley-VCH, New York, 1998).
[2] Á. Kvaran, H. Wang, and Á. Logadóttir, in *Recent Research Developments in Physical Chemistry*, Vol. 2 (Transworld Research Network, India, 1998), p. 233.
[3] W. Huasheng, J. Ásgeirsson, Á. Kvaran, R. J. Donovan, R. V. Flood, K. P. Lawley, T. Ridley, and A. J. Yencha, J. Mol. Struct. **293**, 217 (1993).
[4] Á. Kvaran, H. Wang, and J. Ásgeirsson, J. Mol. Spectrosc. **163**, 541 (1994).
[5] Á. Kvaran, H. Wang, G. H. Jóhannesson, and A. J. Yencha, Chem. Phys. Lett. **222**, 436 (1994).
[6] Á. Kvaran, G. H. Jóhannesson, and H. Wang, Chem. Phys. **204**, 65 (1996).
[7] G. H. Jóhannesson, H. Wang, and Á. Kvaran, J. Mol. Spectrosc. **179**, 334 (1996).
[8] Á. Kvaran, H. Wang, and G. H. Jóhannesson, J. Phys. Chem. **99**, 4451 (1995).
[9] Á. Kvaran, Á. Logadóttir, and H. Wang, J. Chem. Phys. **109**, 5856 (1998).
[10] E. de Beer, B. G. Koenders, M. P. Koopmans, and C. A. de Lange, J. Chem. Soc., Faraday Trans. **86**, 2035 (1990).
[11] Y. Xie, P. T. A. Reilly, S. Chilukuri, and R. J. Gordon, J. Chem. Phys. **95**, 854 (1991).
[12] D. S. Green and S. C. Wallace, J. Chem. Phys. **96**, 5857 (1992).
[13] D. S. Green, G. A. Bickel, and S. C. Wallace, J. Mol. Spectrosc. **150**, 303 (1991).
[14] D. S. Green, G. A. Bickel, and S. C. Wallace, J. Mol. Spectrosc. **150**, 354 (1991).
[15] D. S. Green, G. A. Bickel, and S. C. Wallace, J. Mol. Spectrosc. **150**, 388 (1991).
[16] R. Callaghan and R. J. Gordon, J. Chem. Phys. **93**, 4624 (1990).
[17] S. A. Wright and J. D. McDonald, J. Chem. Phys. **101**, 238 (1994).
[18] S. T. Pratt and M. L. Ginter, J. Chem. Phys. **102**, 1882 (1995).
[19] C. R. Scheper, W. J. Buma, C. A. de Lange, and W. J. van der Zande, J. Chem. Phys. **109**, 8319 (1998).
[20] B. R. Lewis, S. T. Gibson, R. A. Copeland, and C. G. Bressler, Phys. Rev. Lett. **82**, 4212 (1999).
[21] M. Wu and P. M. Johnson, J. Chem. Phys. **91**, 7399 (1989).
[22] M. R. Dobber, W. J. Buma, and C. A. de Lange, J. Chem. Phys. **101**, 9303 (1994).
[23] C. Cossart-Magos, M. Jungen, and F. Launay, J. Chem. Phys. **109**, 6666 (1998).
[24] C. Cossart-Magos, H. Lefebvre-Brion, M. Jungen, and F. Launay, J. Chem. Phys. **107**, 1308 (1997).
[25] J. P. Berger, S. Couris, and D. Gauyacq, J. Chem. Phys. **107**, 8866 (1997).
[26] B. G. Koenders, D. M. Wieringa, G. J. Kuik, K. E. Drabe, and C. A. de Lange, Chem. Phys. **129**, 41 (1989).
[27] G. Herzberg, *Molecular Spectra and Molecular Structure; I. Spectra of Diatomic Molecules*, 2nd ed. (Van Nostrand Reinhold, New York, 1950).
[28] R. G. Bray and R. M. Hochstrasser, Mol. Phys. **31**, 1199 (1976).
[29] J. B. Halpern, H. Zacharias, and R. Wallenstein, J. Mol. Spectrosc. **79**, 1 (1980).
[30] R. J. Donovan, R. V. Flood, K. P. Lawley, A. J. Yencha, and T. Ridley, Chem. Phys. **164**, 439 (1992).
[31] S. H. Lin, Y. Fujimura, H. J. Neusser, and E. W. Schlag, *Multiphoton Spectroscopy of Molecules* (Academic, New York, 1984).
[32] E. U. Condon and G. H. Shortley, *The Theory of Atomic Spectra* (Cambridge University Press, Cambridge, 1963).
[33] D. L. Falkoff, G. S. Colladay, and R. E. Sells, Can. J. Phys. **30**, 253 (1952).
[34] See EPAPS Document No. E-JCPSA6-113-009029 for (3+1)REMPI spectroscopy of diatomic molecules: Transitions, calculated and experimental spectra for HBr. This document may be retrieved via the EPAPS homepage (http://www.aip.org/pubservs/epaps.html) or from ftp.aip.org in the directory /epaps/. See the EPAPS homepage for more information.
[35] M. L. Ginter and S. G. Tilford, J. Mol. Spectrosc. **34**, 206 (1970).
[36] D. S. Ginter, M. L. Ginter, and S. G. Tilford, J. Mol. Spectrosc. **90**, 152 (1981).
[37] Á. Logadóttir, M.S. thesis, University of Iceland, 1997.